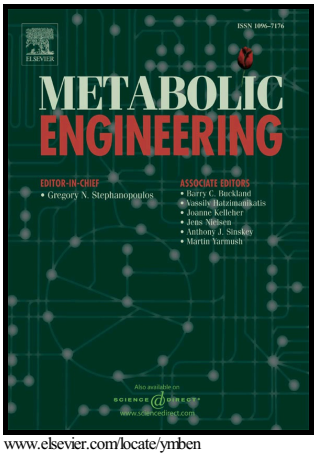

www.elsevier.com/locate/ymben

Metabolism in dense microbial colonies: ^{13}C metabolic flux analysis of *E. coli* grown on agar identifies two distinct cell populations with acetate cross-feeding

Eric Wolfsberg, Christopher P. Long, Maciek R. Antoniewicz

PII: S1096-7176(18)30193-9
DOI: https://doi.org/10.1016/j.ymben.2018.08.013
Reference: YMBEN1461

To appear in: *Metabolic Engineering*

Received date: 9 May 2018
Revised date: 27 July 2018
Accepted date: 31 August 2018

Cite this article as: Eric Wolfsberg, Christopher P. Long and Maciek R. Antoniewicz, Metabolism in dense microbial colonies: ^{13}C metabolic flux analysis of *E. coli* grown on agar identifies two distinct cell populations with acetate cross-feeding, *Metabolic Engineering,* https://doi.org/10.1016/j.ymben.2018.08.013

Metabolism in dense microbial colonies: ^{13}C metabolic flux analysis of *E. coli* grown on agar identifies two distinct cell populations with acetate cross-feeding

Eric Wolfsberg[#], Christopher P. Long[#], Maciek R. Antoniewicz*

Department of Chemical and Biomolecular Engineering, Metabolic Engineering and Systems Biology Laboratory, University of Delaware, Newark DE 19716, USA

[#]these authors contributed equally

*corresponding author:

Maciek R. Antoniewicz

Department of Chemical and Biomolecular Engineering

University of Delaware

150 Academy St, Newark, DE 19716

Tel.: 302-831-8960, Fax.: 302-831-1048

Email: mranton@udel.edu

ABSTRACT

In this study, we have investigated for the first time the metabolism of *E. coli* grown on agar using ^{13}C metabolic flux analysis (^{13}C-MFA). To date, all ^{13}C-MFA studies on microbes have been performed with cells grown in liquid culture. Here, we extend the scope of ^{13}C-MFA to biological systems where cells are grown in dense microbial colonies. First, we identified new optimal ^{13}C tracers to quantify fluxes in systems where the acetate yield cannot be easily measured. We determined that three parallel labeling experiments with the tracers [1,2-^{13}C]glucose, [1,6-^{13}C]glucose, and [4,5,6-^{13}C]glucose permit precise estimation of not only intracellular fluxes, but also of the amount of acetate produced from glucose. Parallel labeling experiments were then performed with wild-type *E. coli* and *E. coli* Δ*ackA* grown in liquid culture and on agar plates. Initial attempts to fit the labeling data from wild-type *E. coli* grown on agar did not produce a statistically acceptable fit. To resolve this issue, we employed the recently developed co-culture ^{13}C-MFA approach, where two *E. coli* subpopulations were defined in the model that engaged in metabolite cross-feeding. The flux results identified two distinct *E. coli* cell populations, a dominant cell population (92% of cells) that metabolized glucose via conventional metabolic pathways and secreted a large amount of acetate (~40% of maximum theoretical yield), and a second smaller cell population (8% of cells) that consumed the secreted acetate without any glucose influx. These experimental results are in good agreement with recent theoretical simulations. Importantly, this study provides a solid foundation for future investigations of a wide range of problems involving microbial biofilms that are of great interest in biotechnology, ecology and medicine, where metabolite cross-feeding between cell populations is a core feature of the communities.

Graphical abstract

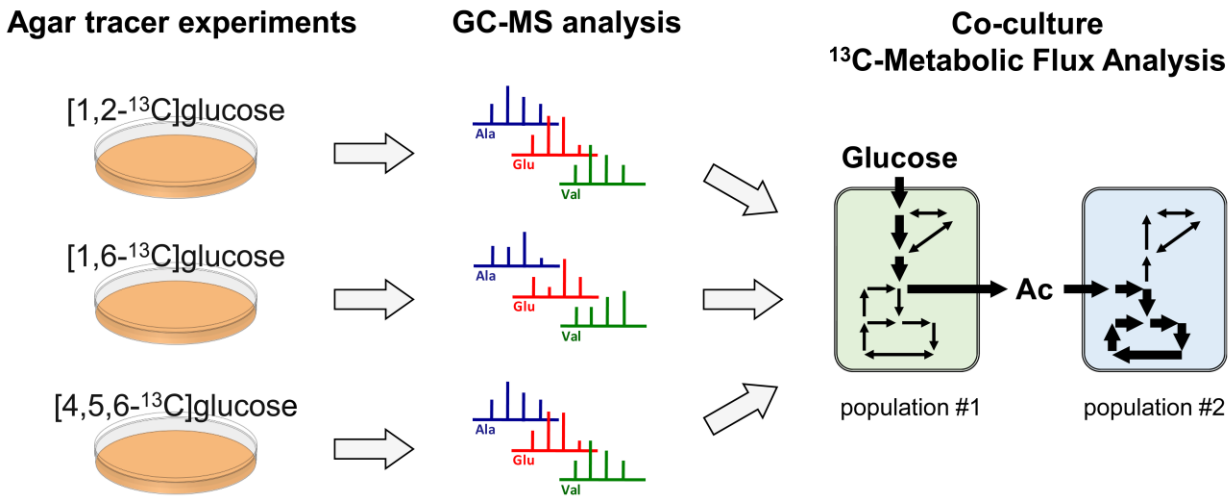

KEYWORDS

Escherichia coli, bacterial colonies, biofilm, metabolite exchange, cross-feeding, microbial communities.

1. INTRODUCTION

^{13}C metabolic flux analysis (^{13}C-MFA) is a powerful and widely used technique in metabolic engineering to quantify intracellular metabolic rates, i.e. metabolic fluxes, in living systems (Gonzalez and Antoniewicz, 2017; Stephanopoulos, 1999). After two decades of development and application, the ^{13}C-MFA methodology is now firmly established as a cornerstone of

metabolic engineering practice (Crown and Antoniewicz, 2013). The most common application of ^{13}C-MFA involves growing a single microbial strain in batch culture (or continuous culture) in the presence of a glucose tracer, e.g. [1,2-^{13}C]glucose, measuring isotopic labeling in proteinogenic amino acids, determining external rates (e.g. glucose uptake and acetate secretion rates), and then fitting the data to a metabolic model to estimate intracellular fluxes. In addition to investigations of model and non-model microbial systems (Long and Antoniewicz, 2014a; Swarup et al., 2014), ^{13}C-MFA is now also routinely applied to investigate metabolism of mammalian cells (Antoniewicz, 2018; Young, 2013). An important recent advance in ^{13}C-MFA has been the use of parallel labeling experiments (Crown et al., 2015), which has greatly improved the precision and accuracy of estimated fluxes and has enabled the discovery of new metabolic pathways (Ahn et al., 2016).

In this contribution, we extend the ^{13}C-MFA methodology to include investigations of metabolic fluxes and metabolic interactions (i.e. metabolite cross-feeding) in dense microbial colonies. Specifically, in this study we have investigated for the first time the metabolism of *E. coli* grown on glucose minimal agar plates. Recent theoretical studies using a multi-scale flux balance analysis approach, called 3-dimensional dynamic flux balance analysis (3DdFBA), have suggested that within dense *E. coli* colonies two metabolically distinct subpopulations are expected to naturally emerge and engage in cooperative acetate cross-feeding (Cole et al., 2015; Peterson et al., 2017). Depending on the location within a colony, some cells will experience a glucose-rich environment that promotes acetate-producing fermentative metabolism, while other cells will experience a glucose-deprived environment that promotes acetate consumption. Simulation results have suggested that for wild-type *E. coli*, the relative fraction of acetate-

utilizing cells within the colonies would be around 5-10% (Peterson et al., 2017). In this work, we optimized ^{13}C-tracer experiments and employed a co-culture ^{13}C-MFA methodology (Gebreselassie and Antoniewicz, 2015) to validate these predictions experimentally. Taken together, our work paves the way for future ^{13}C-flux studies of complex microbial communities in biofilms. To date, limitations in experimental and analytical approaches have greatly restricted *in vivo* investigations of metabolic phenotypes and metabolic interactions in this important context.

2. MATERIALS AND METHODS

2.1. Materials

Chemicals and media were purchased from Sigma-Aldrich (St. Louis, MO). Isotopic tracers were purchased from Cambridge Isotope Laboratories (Tewksbury, MA): [1,2-^{13}C]glucose (99.9 %), [1,6-^{13}C]glucose (98.8 % ^{13}C), [4,5,6-^{13}C]glucose (99.6 % ^{13}C), and [U-^{13}C]glucose (98.9 % ^{13}C). The isotopic purity of glucose tracers were verified by GC-MS analysis as described in (Sandberg et al., 2016). All solutions were sterilized by filtration.

2.2. Strains and growth conditions

Wild-type *E. coli* BW25113 and *E. coli* Δ*ackA* were obtained from the Keio collection (GE Healthcare Dharmacon, Cat. No. OEC5042). For liquid cultures, *E. coli* was first grown overnight in M9 minimal medium with 2 g/L of unlabeled glucose. Next, 100 µL of this preculture was used to inoculate 10 mL of M9 minimal medium with 2 g/L of ^{13}C-labeled

glucose. Cells were cultured aerobically at 37°C in parallel mini-bioreactors with 10 mL working volume (Long et al., 2017b). Three labeling experiments were performed in parallel, with [1,2-^{13}C]glucose, [1,6-^{13}C]glucose, and [4,5,6-^{13}C]glucose. Cells were harvested for GC-MS analysis during the mid-exponential growth when OD_{600} was approximately 0.7. For agar cultures, *E. coli* was first grown overnight in M9 minimal medium with 2 g/L of unlabeled glucose. Next, 10 µL of this preculture was pipetted onto an agar plate (M9 minimal medium + 15 g/L agar + 2 g/L ^{13}C-labeled glucose) and spread over the entire agar plate using a sterile L-shaped cell spreader. After 18 hr incubation at 37°C in a humidified incubator the cells were collected with a cell scraper, re-dissolved in 1 mL of glucose-free M9 medium, and centrifuged to obtain a cell pellet for subsequent GC-MS analysis.

2.3. Analytical methods

Cell growth in liquid cultures was monitored by measuring the optical density at 600nm (OD_{600}) using a spectrophotometer (Eppendorf BioPhotometer). The OD_{600} values were converted to cell dry weight concentrations using a previously determined OD_{600}-dry cell weight relationship for *E. coli* (1.0 OD_{600} = 0.32 g_{DW}/L) (Long et al., 2016b). Acetate concentrations in supernatants were determined using an Agilent 1200 Series HPLC (Gonzalez et al., 2017). Glucose concentrations were determined using a YSI 2700 biochemistry analyzer (YSI, Yellow Springs, OH). The yield of acetate on glucose was calculated from linear regression of the measured acetate and glucose concentrations during the exponential growth phase.

2.4. Gas chromatography-mass spectrometry

GC-MS analysis was performed on an Agilent 7890B GC system equipped with a DB-5MS capillary column (30 m, 0.25 mm i.d., 0.25 µm-phase thickness; Agilent J&W Scientific), connected to an Agilent 5977A Mass Spectrometer operating under ionization by electron impact (EI) at 70 eV. Helium flow was maintained at 1 mL/min. The source temperature was maintained at 230°C, the MS quad temperature at 150°C, the interface temperature at 280°C, and the inlet temperature at 250°C. GC-MS analysis of *tert*-butyldimethylsilyl (TBDMS) derivatized proteinogenic amino acids was performed as described in (Long and Antoniewicz, 2014b). Labeling of glucose (derived from glycogen) and ribose (derived from RNA) were determined as described in (Long et al., 2016a; McConnell and Antoniewicz, 2016). In all cases, mass isotopomer distributions were obtained by integration and corrected for natural isotope abundances (Fernandez et al., 1996).

2.5. ^{13}C metabolic flux analysis

^{13}C-MFA calculations were performed using the Metran software, which is based on the elementary metabolite units (EMU) framework (Antoniewicz et al., 2007a). Fluxes were estimated by minimizing the variance-weighted sum of squared residuals (SSR) between the measured and model predicted mass isotopomer distributions using non-linear least-squares regression. The metabolic network used for ^{13}C-MFA is based on the *E. coli* model described previously (Long et al., 2018), which includes all major metabolic pathways of central carbon metabolism, lumped amino acid biosynthesis reactions and a lumped biomass formation reaction. The model also accounts for the dilution of intracellular CO_2 by unlabeled (atmospheric) carbon dioxide as described in (Gonzalez et al., 2017). An update to the model includes making the reaction between PEP and pyruvate reversible based on the results described in (Long et al.,

2017a). For co-culture ^{13}C-MFA, two compartmentalized *E. coli* models were fitted simultaneously as described in (Gebreselassie and Antoniewicz, 2015). In addition to the flux parameters, the co-culture model also contained a parameter that described the relative population sizes (in each experimental data set) (Gebreselassie and Antoniewicz, 2015), and a reaction to describe cross-feeding of acetate between the cell populations.

All measured mass isotopomers used for ^{13}C-MFA are provided in Supplemental Materials. For integrated analysis of parallel labeling experiments, the three data sets were fitted simultaneously as described in (Antoniewicz, 2015). Flux estimation was repeated 10 times starting with random initial values for all fluxes to find a global solution. At convergence, accurate 95% confidence intervals were computed for all estimated fluxes by evaluating the sensitivity of the minimized SSR to flux variations. Precision of estimated fluxes was determined as follows (Antoniewicz et al., 2006):

$$\text{Flux precision (stdev)} = [(\text{flux}_{\text{upper bound 95\%}}) - (\text{flux}_{\text{lower bound 95\%}})] / 4$$

To describe fractional labeling of metabolites, G-value parameters were included in ^{13}C-MFA. As described previously (Antoniewicz et al., 2007b), the G-value represents the fraction of a metabolite pool that is produced during the labeling experiment, while 1-G represents the fraction that is naturally labeled (i.e. from the inoculum). By default, one G-value parameter was included for each measured metabolite in each data set. Reversible reactions were modeled as

separate forward and backward fluxes. Net and exchange fluxes were determined as follows: $v_{net} = v_f - v_b$; $v_{exch} = \min(v_f, v_b)$.

2.6. Goodness-of-fit analysis

To determine the goodness-of-fit, ^{13}C-MFA fitting results were subjected to a χ^2-statistical test. In short, assuming that the model is correct and data are without gross measurement errors, the minimized SSR is a stochastic variable with a χ^2-distribution (Antoniewicz et al., 2006). The number of degrees of freedom is equal to the number of fitted measurements *n* minus the number of estimated independent parameters *p*. The acceptable range of SSR values is between $\chi^2_{\alpha/2}(n-p)$ and $\chi^2_{1-\alpha/2}(n-p)$, where α is a certain chosen threshold value, for example 0.05 for 95% confidence interval.

3. RESULTS AND DISCUSSION

3.1. Optimal tracers to estimate the acetate yield

In traditional ^{13}C-MFA, intracellular fluxes are quantified by fitting isotopic labeling measurements (e.g. GC-MS data) and external rate measurements (e.g. glucose uptake rate, acetate secretion rate, and growth rate) to a metabolic model. External rates are important inputs for ^{13}C-MFA since isotopic labeling measurements by themselves only provide relative flux information. In liquid cultures, external rates are easily determined by measuring the concentrations of biomass, glucose and acetate over time from which external rates can be calculated in a straightforward way by linear regression, typically expressed in units mmol/g_{DW}/h. Alternatively, if fluxes are normalized to glucose uptake rate, then the acetate yield

(expressed as mols of acetate produced per mols of glucose consumed) is used as an external constraint in ^{13}C-MFA.

However, for cells grown on agar there is no easy method to determine the amount of glucose consumed or the amount of acetate produced, thus making it difficult to apply the traditional ^{13}C-MFA approach to determine precise metabolic fluxes. To address this limitation, we first investigated if it would be possible to design a set of tracer experiments such that the acetate yield could be determined from labeling data alone, thus eliminating the need to measure the acetate yield experimentally. To identify optimal tracers, we performed extensive *in silico* ^{13}C-MFA simulations using the approach described in (Crown et al., 2016).

First, we evaluated all possible single glucose tracers, assuming that typical GC-MS measurements of proteinogenic amino acids can be performed. The simulation results suggested that there was no single glucose tracer that would allow the acetate yield to be determined with precision. Next, we evaluated all possible dual parallel labeling experiments. In this case, we identified several combinations of two glucose tracers that could estimate the acetate yield, although with a fairly poor precision of about 25%. Next, we evaluated all possible triple parallel labeling experiments. In this case, we found several combinations of three glucose tracers that allowed the acetate yield to be estimated with high precision, i.e. with standard deviation less than 7%. Overall, the best combination of three parallel labeling experiments involved the following three glucose tracers: [1,2-^{13}C]glucose, [1,6-^{13}C]glucose and [4,5,6-^{13}C]glucose.

To validate this experimental design, wild-type *E. coli* and *E. coli* Δ*ackA* were grown in three parallel liquid cultures with the three optimal tracers, i.e. [1,2-^{13}C]glucose, [1,6-^{13}C]glucose and [4,5,6-^{13}C]glucose. Isotopic labeling was measured by GC-MS and the data was fit to an *E. coli* network model. No acetate flux was specified as a constraint for ^{13}C-MFA. Fitting the isotopic labeling data from the three parallel labeling experiments resulted in statistically acceptable fits with a sum of squared residuals (SSR) value of 322 for wild-type *E. coli* and 184 for *E. coli* Δ*ackA*, both of which were lower than the maximum acceptable SSR value of 385 at 95% confidence level. The complete flux results, including 95% confidence intervals are given in Supplemental Materials. The estimated acetate yield for wild-type *E. coli* was 0.64 ± 0.06 mol/mol, which was in good agreement with the experimentally determined acetate yield of 0.71 ± 0.05 (Table 1). For *E. coli* Δ*ackA*, the ^{13}C-MFA estimated acetate yield of 0.22 ± 0.07 mol/mol was also in good agreement with the experimentally measured yield of 0.19 ± 0.04 mol/mol. Furthermore, the estimated metabolic fluxes for wild-type *E. coli* were in good agreement with previously reported fluxes for this strain (Long et al., 2018). No comparison could be made with previous reports for *E. coli* Δ*ackA*, since this is the first time that ^{13}C-MFA was applied to this strain. The low acetate yield of *E. coli* Δ*ackA* was expected based on previous reports (Enjalbert et al., 2017). Overall, these results verify that parallel labeling experiments with [1,2-^{13}C]glucose, [1,6-^{13}C]glucose and [4,5,6-^{13}C]glucose produce accurate and precise values for both the acetate yield and intracellular metabolic fluxes.

3.2. Validation of labeling incorporation for *E. coli* grown on agar

Before performing parallel labeling experiments with *E. coli* grown on agar, we first set out to validate that we can achieve complete ^{13}C-labeling of *E. coli* biomass when cells are cultured on agar containing 2 g/L of [U-^{13}C]glucose. Specifically, we wanted to validate that no unlabeled components from the agar would be metabolized by *E. coli*, as this would result in reduced ^{13}C-labeling that would need to be accounted for in the model. Fig. 1 shows the measured isotopic labeling of amino acids from hydrolyzed biomass for wild-type *E. coli* grown on [U-^{13}C]glucose minimal agar plates. For most amino acids we observed the expected amount of ^{13}C-labeling, with the main ion being the fully labeled mass isotopomer M+*N*, where *N* is the number of C-atoms of a specific amino acid fragment. Since the [U-^{13}C]glucose tracer was not 100% labeled (i.e. we determined that the tracer used had an isotopic purity of 98.9 atom% ^{13}C), some incompletely labeled mass isotopomers (M+*N*-1) were expected and were also observed (Fig. 1). For aspartate, glutamate and several amino acids we observed higher than expected abundances of M+*N*-1 mass isotopomers. In a previous study using *E. coli* grown in liquid culture on [U-^{13}C]glucose (Leighty and Antoniewicz, 2012), we observed similar dilutions of labeling for these amino acids which could be explained by the incorporation of unlabeled (atmospheric) CO_2 via the anaplerotic reaction: phosphoenolpyruvate + $CO_2 \rightarrow$ oxaloacetate (i.e. oxaloacetate is the precursor for aspartate, glutamate and several related amino acids). Thus, the partial labeling observed for these amino acids is not related to the utilization of components from the agar, but results from the incorporation of unlabeled atmospheric CO_2, which is already accounted for in our *E. coli* model.

3.3. Co-culture ^{13}C-MFA of *E. coli* grown on agar

Next, we performed parallel labeling experiments with wild-type *E. coli* and *E. coli* Δ*ackA* on glucose minimal agar plates with the three optimal glucose tracers, [1,2-^{13}C]glucose, [1,6-^{13}C]glucose and [4,5,6-^{13}C]glucose. Isotopic labeling of proteinogenic amino acids was measured by GC-MS and the data were fit to an *E. coli* network model. For *E. coli* Δ*ackA*, we obtained a statistically acceptable fit with an SSR value of 307. However, the fit for wild-type *E. coli* was not statistically acceptable with an SSR value of 826, which was much higher than the maximum acceptable SSR value of 385 at 95% confidence level (Figure 2).

A previous 3DdFBA simulation study suggested that wild-type *E. coli* when grown on agar would naturally separate into two distinct cell populations (Cole et al., 2015): one population that is closest to the agar which grows on glucose and secretes acetate, and a second population that grows on top of the first population and utilizes the secreted acetate as a carbon source (Cole et al., 2015). By applying microscopy imaging, qualitative support for these predictions was provided by the authors (Cole et al., 2015). Here, we set out to test these predictions using ^{13}C-MFA. For this, the labeling data from the parallel labeling experiments were fit to two versions of a co-culture model, with and without acetate cross-feeding (Fig 2). To perform co-culture flux analysis, we used the same framework as was recently developed for analysis of microbial co-cultures grown in liquid culture (Gebreselassie and Antoniewicz, 2015). The co-culture model consisted of two compartmentalized *E. coli* models, each containing the complete set of *E. coli* metabolic reactions, as well as a parameter that estimated the fraction of each cell population in the sample. For technical details regarding how co-culture ^{13}C-MFA was performed, the reader is referred to the detailed description in (Gebreselassie and Antoniewicz, 2015). Fitting the labeling data from the parallel labeling experiments to the co-culture model without acetate cross-feeding

did not produce a statistically acceptable fit. However, fitting the data to the co-culture model with acetate cross-feeding did produce an acceptable fit with an SSR value of 350.

The estimated metabolic fluxes for wild-type *E. coli* and *E. coli* Δ*ackA* grown on agar plates and in liquid culture are shown schematically in Fig. 3. The complete flux results, including 95% confidence intervals are given in Supplemental Materials. The fluxes for *E. coli* Δ*ackA* grown in liquid culture and on agar plates were very similar. As expected, the amount of glucose converted to acetate was small in both cases (22 ± 7 for liquid culture and 25 ± 11 for agar plates, normalized to glucose uptake of 100). In fact, the only significant flux change was a ~30% increase in TCA cycle fluxes and a slight increase in malic enzyme flux (2 ± 1 for liquid culture vs. 8 ± 2 for agar culture). The fact that the mono-culture model was able to describe the labeling data for *E. coli* Δ*ackA* was expected, since it is well known that this strain produces only small amounts of acetate and is unable to uptake acetate (Enjalbert et al., 2017). Thus, for this strain there was no opportunity for two cell populations to emerge and engage in acetate cross-feeding.

For wild-type *E. coli* grown on agar, the co-culture ^{13}C-MFA methodology estimated precise fluxes for the two phenotypically distinct *E. coli* cell populations. There was a dominant *E. coli* population (92% ± 0.4% of cells) that utilized glucose as the carbon source and secreted acetate as the by-product, and a second smaller population that only utilized acetate for cell growth without any glucose influx. The amount of acetate produced from glucose was relatively high for the first cell population, i.e. 120 ± 1 mols of acetate produced per 100 mols of glucose

consumed, which is about twice as much acetate produced from glucose compared to *E. coli* grown in liquid culture (64 ± 6). Correspondingly, the biomass yield on agar was approximately half that in liquid culture (0.21 ± 0.01 vs. 0.44 ± 0.02 g_{DW}/g_{gluc}). Interestingly, many core metabolic fluxes were very similar for *E. coli* grown in liquid culture and on agar plates (Fig. 3), where about 2/3 of glucose was metabolized via glycolysis, 1/3 via pentose phosphate pathway, and no flux through the ED pathway. The TCA cycle fluxes were also very similar; for example, the citrate synthase flux for *E. coli* grown on agar was 17 ± 1 compared to 19 ± 1 for *E. coli* grown in liquid culture.

The second (smaller) *E. coli* population from the agar cultures with wild-type *E. coli* (8% ± 0.4% of cells) utilized acetate as the only carbon source. Although our model contained reactions for both glucose and acetate influx, the estimated glucose uptake rate was negligible (0 ± 0.4) normalized to acetate uptake of 100. The ^{13}C-flux results further suggested that the majority of acetate was catabolized in the TCA cycle to CO_2 and that only a small fraction was used for cell growth via glyoxylate shunt. The ^{13}C-MFA estimated fraction of acetate-consuming cells (8% ± 0.4%) was in good agreement with recent theoretical 3DdFBA simulations, where the relative fraction of acetate-utilizing cells within a fully developed *E. coli* colony was predicted to be around 5-10% for wild-type *E. coli* (Peterson et al., 2017).

4. CONCLUSIONS

In this work, we have investigated for the first time the metabolism of *E. coli* cells grown on agar. First, a new set of optimal parallel labeling experiments was designed that allowed us to determine not only intracellular metabolic fluxes with high precision, but also to quantify acetate

production from glucose using only isotopic labeling data as the input. To validate this new methodology, we showed that the estimated acetate yield for two *E. coli* strains grown in liquid culture was the same as the directly measured acetate yield. Next, this approach was applied to investigate metabolism of *E. coli* grown on agar. We used statistical analysis of the flux fits to demonstrate that wild-type *E. coli* formed two distinct cell populations that engaged in acetate cross-feeding. To obtain these results, we leveraged the recently developed co-culture ^{13}C-MFA framework that can estimate precise metabolic fluxes for multiple cell populations without the need for physical separation of cells (Gebreselassie and Antoniewicz, 2015).

Overall, the key contribution of this work is in extending the scope of ^{13}C-MFA studies to a wide range of new systems that were previously inaccessible to experimental fluxomic approaches. Given the importance of biofilms in many biological systems of relevance to biotechnology, ecology and medicine (Arrigo, 2005; Eckburg et al., 2005), we anticipate that the methods developed in this work will be valuable in generating new knowledge and insights into the physiology and metabolism of cells interacting in biofilms (Ben-Jacob et al., 1998; Harcombe et al., 2014).

In future work, it will be valuable to explore the limits of the framework developed in this study. For example, the following questions could be addressed: is it possible to identify additional metabolic phenotypes (i.e., more than two subpopulations as described here) if additional tracer experiments and/or labeling measurements are included? Is it possible to identify cells that switch between glucose consumption and acetate consumption over time? Can the methodology be applied to study metabolism of non-growing (dormant) cells? At some level of precision there

is almost certainly more spatiotemporal complexity than the two homogenous populations that we have characterized here. Further development of this framework may be able address some or all of these questions.

ACKNOWLEDGEMENTS

This work was supported by NSF MCB-1616332 grant.

TABLES

Table 1. Comparison of directly measured acetate yield and ^{13}C-MFA estimated acetate yield.

Strain	Measured acetate yield (mol/mol)	^{13}C-MFA estimated acetate yield (mol/mol)*
Wild-type *E. coli*	0.71 ± 0.05	0.64 ± 0.06
E. coli Δ*ackA*	0.19 ± 0.04	0.22 ± 0.07

* Acetate yield was estimated using ^{13}C-MFA by simultaneously fitting GC-MS measurements from three parallel labeling experiments, with [1,2-^{13}C]glucose, [1,6-^{13}C]glucose and [4,5,6-^{13}C]glucose.

FIGURE LEGENDS

Figure 1. Expected (black bars) and measured (red bars) mass isotopomer distributions for four biomass amino acids (histidine, valine, aspartate, and glutamate) from *E. coli* grown on [U-^{13}C]glucose minimal agar plate. The presence of incompletely labeled mass isotopomers for aspartate (M+3) and glutamate (M+4) suggests incorporation of unlabeled atmospheric CO_2. Mass isotopomers were corrected for natural isotope abundances.

Figure 2. Statistical analysis of the goodness-of-fit. ^{13}C-MFA was performed by simultaneously fitting GC-MS measurements from three parallel labeling experiments with the optimal glucose tracers [1,2-^{13}C]glucose, [1,6-^{13}C]glucose and [4,5,6-^{13}C]glucose. (A) Three different metabolic models were evaluated, a traditional mono-culture model, a co-culture model without metabolite cross-feeding, and a co-culture model with acetate cross-feeding. (B) The mono-culture model was sufficient to yield a statistically acceptable fit for wild-type *E. coli* grown in liquid culture and *E. coli* Δ*ackA* grown in liquid culture and on agar plates. For wild-type *E. coli* grown on agar plates, only the co-culture model with acetate cross-feeding produced a statistically acceptable fit.

Figure 3. Metabolic flux maps for wild-type *E. coli* and *E. coli* Δ*ackA* grown in liquid culture and on agar plates (best fit ± stdev). Fluxes were determined using ^{13}C-MFA by simultaneously fitting GC-MS measurements from three parallel labeling experiments with the optimal glucose tracers [1,2-^{13}C]glucose, [1,6-^{13}C]glucose and [4,5,6-^{13}C]glucose. For wild-type *E. coli* grown on agar the co-culture ^{13}C-MFA framework was used to estimate fluxes for two phenotypically

distinct cell populations. Fluxes were normalized to the influx of the main carbon source. The complete flux results are provided in Supplemental Materials.

REFERENCES

Ahn, W. S., Crown, S. B., Antoniewicz, M. R., 2016. Evidence for transketolase-like TKTL1 flux in CHO cells based on parallel labeling experiments and (13)C-metabolic flux analysis. Metab Eng. 37**,** 72-8.

Antoniewicz, M. R., 2015. Parallel labeling experiments for pathway elucidation and 13C metabolic flux analysis. Curr Opin Biotechnol. 36**,** 91-97.

Antoniewicz, M. R., 2018. A guide to (13)C metabolic flux analysis for the cancer biologist. Experimental & molecular medicine. 50**,** 19.

Antoniewicz, M. R., Kelleher, J. K., Stephanopoulos, G., 2006. Determination of confidence intervals of metabolic fluxes estimated from stable isotope measurements. Metab Eng. 8**,** 324-37.

Antoniewicz, M. R., Kelleher, J. K., Stephanopoulos, G., 2007a. Elementary metabolite units (EMU): a novel framework for modeling isotopic distributions. Metab Eng. 9**,** 68-86.

Antoniewicz, M. R., Kraynie, D. F., Laffend, L. A., Gonzalez-Lergier, J., Kelleher, J. K., Stephanopoulos, G., 2007b. Metabolic flux analysis in a nonstationary system: fed-batch fermentation of a high yielding strain of E. coli producing 1,3-propanediol. Metab Eng. 9**,** 277-92.

Arrigo, K. R., 2005. Marine microorganisms and global nutrient cycles. Nature. 437**,** 349-55.

Ben-Jacob, E., Cohen, I., Gutnick, D. L., 1998. Cooperative organization of bacterial colonies: from genotype to morphotype. Annual review of microbiology. 52**,** 779-806.

Cole, J. A., Kohler, L., Hedhli, J., Luthey-Schulten, Z., 2015. Spatially-resolved metabolic cooperativity within dense bacterial colonies. BMC Syst Biol. 9**,** 15.

Crown, S. B., Antoniewicz, M. R., 2013. Publishing 13C metabolic flux analysis studies: a review and future perspectives. Metab Eng. 20**,** 42-8.

Crown, S. B., Long, C. P., Antoniewicz, M. R., 2015. Integrated 13C-metabolic flux analysis of 14 parallel labeling experiments in Escherichia coli. Metab Eng. 28**,** 151-8.

Crown, S. B., Long, C. P., Antoniewicz, M. R., 2016. Optimal tracers for parallel labeling experiments and 13C metabolic flux analysis: A new precision and synergy scoring system. Metab Eng. 38**,** 10-18.

Eckburg, P. B., Bik, E. M., Bernstein, C. N., Purdom, E., Dethlefsen, L., Sargent, M., Gill, S. R., Nelson, K. E., Relman, D. A., 2005. Diversity of the human intestinal microbial flora. Science. 308**,** 1635-8.

Enjalbert, B., Millard, P., Dinclaux, M., Portais, J. C., Letisse, F., 2017. Acetate fluxes in Escherichia coli are determined by the thermodynamic control of the Pta-AckA pathway. Scientific reports. 7**,** 42135.

Fernandez, C. A., Des Rosiers, C., Previs, S. F., David, F., Brunengraber, H., 1996. Correction of 13C mass isotopomer distributions for natural stable isotope abundance. J Mass Spectrom. 31**,** 255-62.

Gebreselassie, N. A., Antoniewicz, M. R., 2015. (13)C-metabolic flux analysis of co-cultures: A novel approach. Metab Eng. 31**,** 132-9.

Gonzalez, J. E., Antoniewicz, M. R., 2017. Tracing metabolism from lignocellulosic biomass and gaseous substrates to products with stable-isotopes. Curr Opin Biotechnol. 43**,** 86-95.

Gonzalez, J. E., Long, C. P., Antoniewicz, M. R., 2017. Comprehensive analysis of glucose and xylose metabolism in Escherichia coli under aerobic and anaerobic conditions by 13C metabolic flux analysis. Metab Eng. 39**,** 9-18.

Harcombe, W. R., Riehl, W. J., Dukovski, I., Granger, B. R., Betts, A., Lang, A. H., Bonilla, G., Kar, A., Leiby, N., Mehta, P., Marx, C. J., Segre, D., 2014. Metabolic resource allocation in individual microbes determines ecosystem interactions and spatial dynamics. Cell Rep. 7**,** 1104-15.

Leighty, R. W., Antoniewicz, M. R., 2012. Parallel labeling experiments with [U-13C]glucose validate E. coli metabolic network model for 13C metabolic flux analysis. Metab Eng. 14**,** 533-41.

Long, C. P., Antoniewicz, M. R., 2014a. Metabolic flux analysis of Escherichia coli knockouts: lessons from the Keio collection and future outlook. Curr Opin Biotechnol. 28**,** 127-33.

Long, C. P., Antoniewicz, M. R., 2014b. Quantifying biomass composition by gas chromatography/mass spectrometry. Anal Chem. 86**,** 9423-7.

Long, C. P., Au, J., Gonzalez, J. E., Antoniewicz, M. R., 2016a. 13C metabolic flux analysis of microbial and mammalian systems is enhanced with GC-MS measurements of glycogen and RNA labeling. Metab Eng. 38**,** 65-72.

Long, C. P., Au, J., Sandoval, N. R., Gebreselassie, N. A., Antoniewicz, M. R., 2017a. Enzyme I facilitates reverse flux from pyruvate to phosphoenolpyruvate in Escherichia coli. Nat Commun. 8**,** 14316.

Long, C. P., Gonzalez, J. E., Cipolla, R. M., Antoniewicz, M. R., 2017b. Metabolism of the fast-growing bacterium Vibrio natriegens elucidated by 13C metabolic flux analysis. Metab Eng. 44**,** 191-197.

Long, C. P., Gonzalez, J. E., Feist, A. M., Palsson, B. O., Antoniewicz, M. R., 2018. Dissecting the genetic and metabolic mechanisms of adaptation to the knockout of a major metabolic enzyme in Escherichia coli. Proc Natl Acad Sci U S A. 115**,** 222-227.

Long, C. P., Gonzalez, J. E., Sandoval, N. R., Antoniewicz, M. R., 2016b. Characterization of physiological responses to 22 gene knockouts in Escherichia coli central carbon metabolism. Metab Eng. 37**,** 102-113.

McConnell, B. O., Antoniewicz, M. R., 2016. Measuring the Composition and Stable-Isotope Labeling of Algal Biomass Carbohydrates via Gas Chromatography/Mass Spectrometry. Anal Chem. 88**,** 4624-8.

Peterson, J. R., Cole, J. A., Luthey-Schulten, Z., 2017. Parametric studies of metabolic cooperativity in Escherichia coli colonies: Strain and geometric confinement effects. PLoS One. 12**,** e0182570.

Sandberg, T. E., Long, C. P., Gonzalez, J. E., Feist, A. M., Antoniewicz, M. R., Palsson, B. O., 2016. Evolution of E. coli on [U-13C]Glucose Reveals a Negligible Isotopic Influence on Metabolism and Physiology. PLoS One. 11**,** e0151130.

Stephanopoulos, G., 1999. Metabolic fluxes and metabolic engineering. Metab Eng. 1**,** 1-11.

Swarup, A., Lu, J., DeWoody, K. C., Antoniewicz, M. R., 2014. Metabolic network reconstruction, growth characterization and 13C-metabolic flux analysis of the extremophile Thermus thermophilus HB8. Metab Eng. 24**,** 173-80.

Young, J. D., 2013. Metabolic flux rewiring in mammalian cell cultures. Curr Opin Biotechnol. 24**,** 1108-15.

Highlights

- Metabolism of *E. coli* grown on agar was investigated using ^{13}C metabolic flux analysis
- Optimal tracers for ^{13}C-MFA are [1,2-^{13}C]glucose, [1,6-^{13}C]glucose, and [4,5,6-^{13}C]glucose
- Within *E. coli* colonies two subpopulations emerge that engage in acetate cross-feeding
- The dominant cell population converts 40% of consumed glucose into secreted acetate
- The second smaller *E. coli* population utilizes acetate as the only carbon source

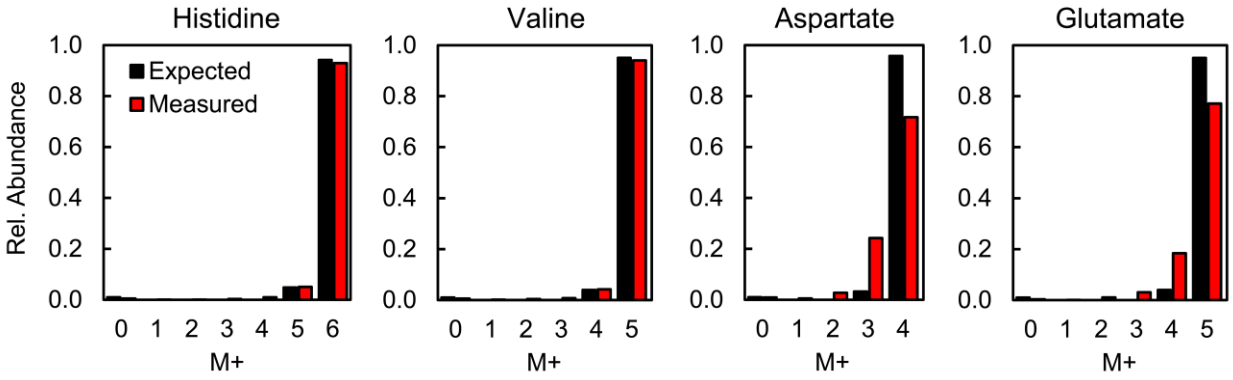

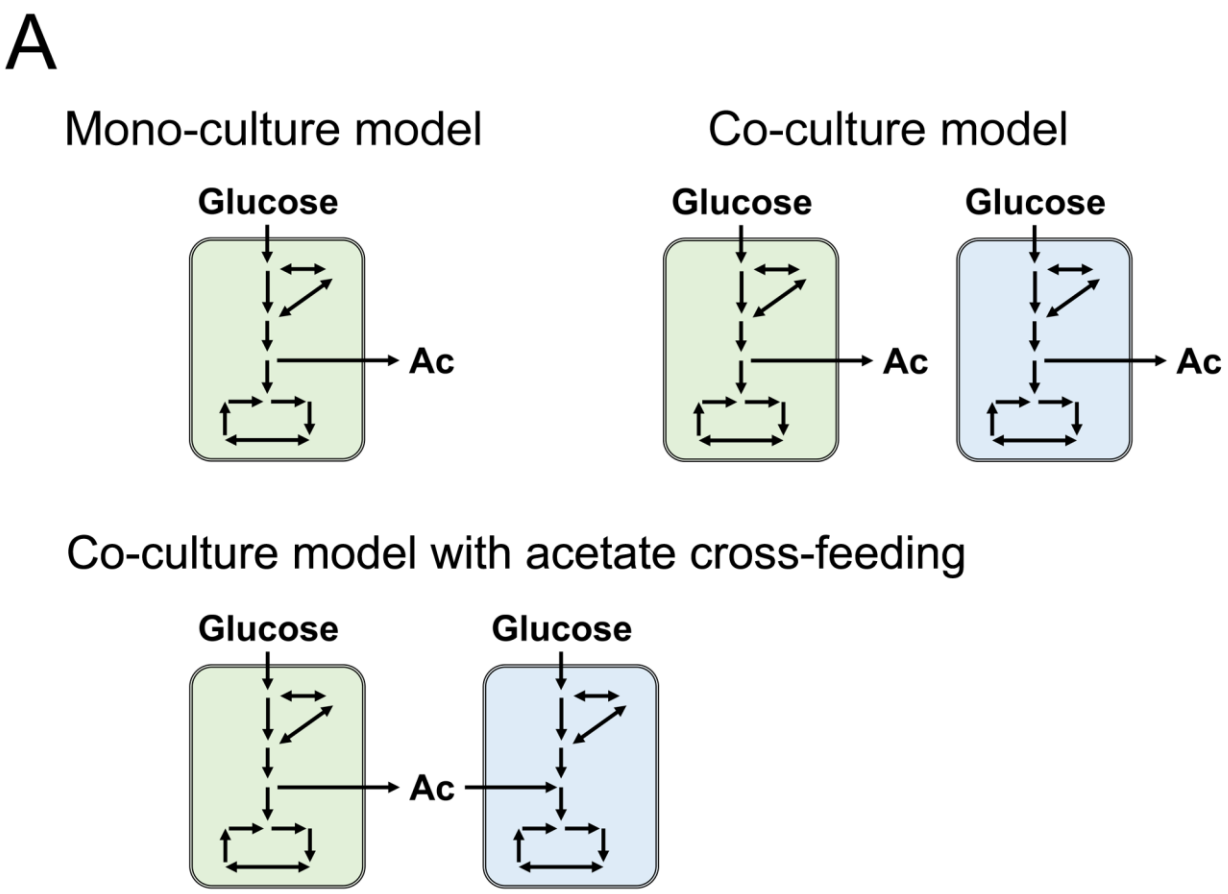
A
Mono-culture model
Glucose
Ac
Co-culture model
Glucose
Ac
Glucose
Ac
Co-culture model with acetate cross-feeding
Glucose
Ac
Glucose
B
SSR
800
600
400
200
0
Mono-culture model
Co-culture model
Co-culture model with acetate exch.
95% Accpt. SSR
WT agar
WT liquid
ΔackA agar
ΔackA liquid

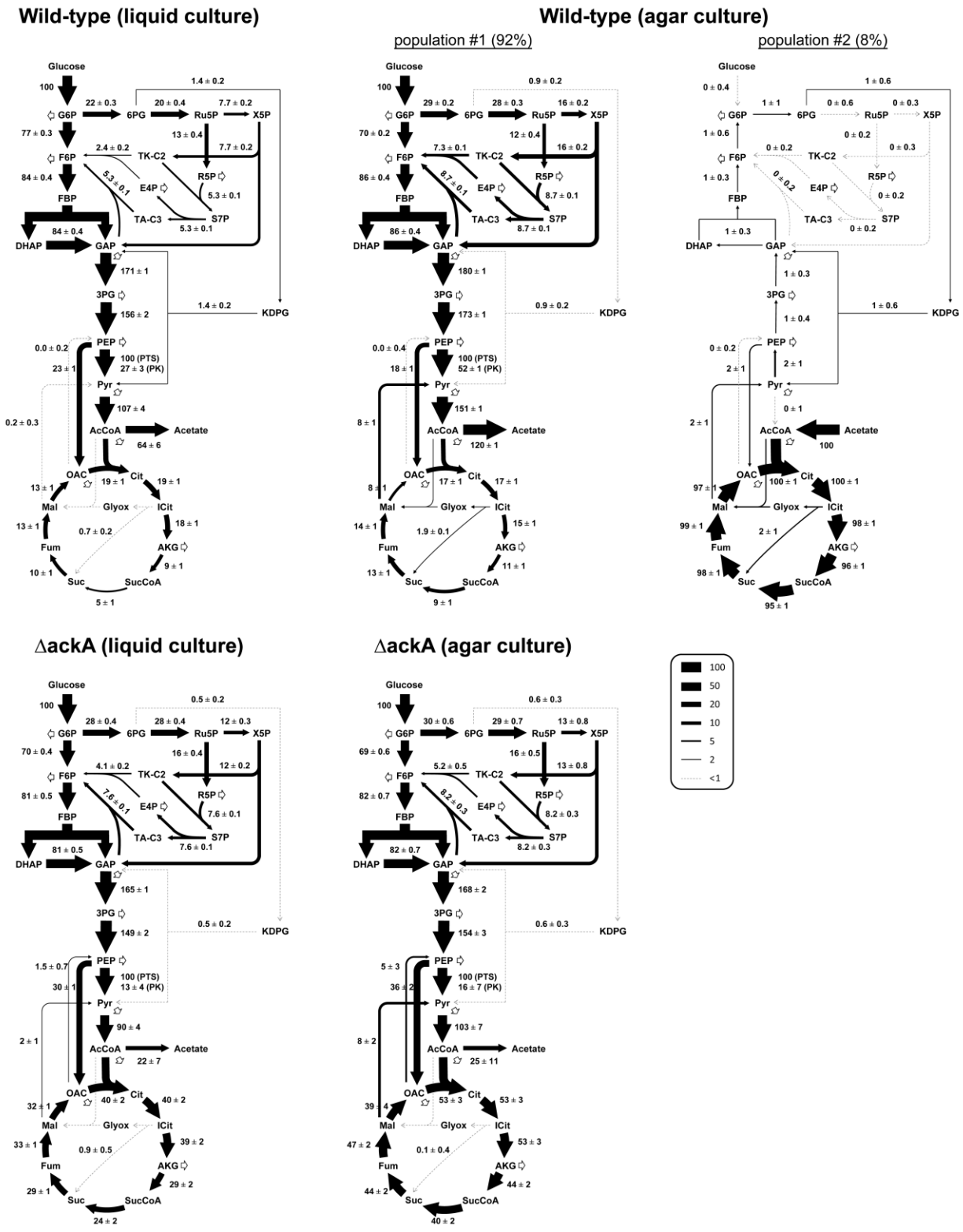
Wild-type (liquid culture)
Wild-type (agar culture)
population #1 (92%)
population #2 (8%)
ΔackA (liquid culture)
ΔackA (agar culture)
Glucose
G6P
6PG
Ru5P
X5P
F6P
TK-C2
R5P
E4P
FBP
TA-C3
S7P
DHAP
GAP
3PG
KDPG
PEP
100 (PTS)
Pyr
AcCoA
Acetate
OAC
Cit
Mal
Glyox
ICit
Fum
AKG
Suc
SucCoA
100
50
20
10
5
2
<1